Statistical Properties of Single Sodium Channels

RICHARD HORN and CAROL A. VANDENBERG

From the Department of Physiology, University of California at Los Angeles School of Medicine, Los Angeles, California 90024

ABSTRACT Single channel currents were obtained from voltage-activated sodium channels in outside-out patches of tissue-cultured GH_3 cells, a clonal line from rat pituitary gland. In membrane patches where the probability of overlapping openings was low, the open time histograms were well fit by a single exponential. Most analysis was done on a patch with exactly one channel. We found no evidence for multiple open states at −25 and −40 mV, since open times, burst durations, and autocorrelation functions were time independent. Amplitude histograms showed no evidence of multiple conductance levels. We fit the gating with 25 different time-homogeneous Markov chain models having up to five states, using a maximum likelihood procedure to estimate the rate constants. For selected models, this procedure yielded excellent predictions for open time, closed time, and first latency density functions, as well as the probability of the channel being open after a step depolarization, the burst duration distribution, autocorrelation, and the distribution of number of openings per record. The models were compared statistically using likelihood ratio tests and Akaike's information criterion. Acceptable models allowed inactivation from closed states, as well as from the open state. Among the models eliminated as unacceptable by this survey were the Hodgkin-Huxley model and any model requiring a channel to open before inactivating.

INTRODUCTION

The mechanisms underlying the voltage-dependent sodium conductance of nerve and muscle have been studied extensively for the last thirty years (for recent reviews, see Armstrong, 1981; Benzanilla, 1982; Brodwick and Eaton, 1982; Yeh, 1982; French and Horn, 1983). The kinetics underlying this time- and voltage-dependent process are quite complex, leading to a wide variety of proposed mechanisms based on observations of macroscopic currents. Until recently, many of these proposals were excessively arbitrary, since it was difficult to systematically eliminate alternative proposals. The advent of gating current and single channel current measurements, however, greatly restricts the possibilities, because these data yield new information that must be consistent with proposed kinetic models.

Address reprint requests to Dr. Richard Horn, Dept. of Physiology, UCLA School of Medicine, Center for the Health Sciences, Los Angeles, CA 90024.

J. GEN. PHYSIOL. © The Rockefeller University Press · 0022-1295/84/10/0505/30 $1.00 505
Volume 84 October 1984 505–534

Kinetic analysis usually involves the construction of a Markov chain model with a finite number of states, and transition rates that are instantaneously voltage dependent. Models of this nature are chosen partly for convenience, but they also have some justification (French and Horn, 1983; for alternative viewpoints, see Neumcke et al., 1978; Greeff et al., 1982; Rubinson, 1982; Fishman et al., 1983). The predictions of a given Markovian model can be compared with experimental data, and models can thus be evaluated. The main purpose of this approach is to estimate parameters of models and eliminate classes of models that are not consistent with experimental data. One hopes that the estimated parameters and acceptable models will give some insight into the molecular processes underlying the gating, and that the kinetic states in such models will be representative of conformational states of the protein molecules responsible for gating.

We have used a statistical approach in examining the single channel behavior of sodium currents from the tissued-cultured cell line GH_3 (Fernandez et al., 1984; Horn et al., 1984). The general questions we ask here are: (*a*) Is the gating process Markovian? (*b*) How many kinetic states are needed to explain sodium channel gating? (*c*) How are the states arranged into a kinetic scheme? (*d*) What are the rate constants between states? (*e*) What is the voltage dependence of each rate constant in the models? We provide partial answers to these questions in this and the accompanying paper (Vandenberg and Horn, 1984). In this paper, we argue that at least one aspect of gating is Markovian and we describe a maximum likelihood analysis of our single channel data using a method developed for estimating parameters and testing hypotheses (Horn and Lange, 1983). We also describe and use procedures for statistically comparing kinetic models. The following paper examines in some detail the interaction between activation and inactivation, and presents evidence that the inactivation process is inherently voltage dependent.

METHODS

The experimental methods have been described previously (Horn et al., 1984) and will be summarized briefly. Single channel records were obtained using outside-out patches from tissue-cultured GH_3 cells, a rat pituitary cell line. The electrodes were fabricated from one of a variety of glasses including Corning 7052 and Corning 8161 (Corning Glass Works, Corning, NY), borosilicate (A-M Systems, Everett, WA), and Vanlab pipettes (VWR, Norwalk, CA). All electrodes were insulated with Sylgard (Sylgard 184; Dow Corning, Midland, MI) and filled with an internal solution consisting of (mM): 120 CsF, 11 EGTA, 2 $MgCl_2$, 1 $CaCl_2$, 10 Cs-HEPES (pH 7.4). The use of CsF was dictated by the following two considerations. (*a*) Inward calcium and outward potassium currents are abolished by this internal solution. This was verified in whole cell recordings, where the subsequent addition of tetrodotoxin abolished all voltage-dependent ionic currents between −70 and +60 mV. (*b*) The patches were very stable in this solution, often lasting >2 h. The bath contained 160 NaCl, 2 $CaCl_2$, 1 $MgCl_2$, and 10 Na-HEPES (pH 7.4). Voltages were corrected for a measured liquid junction potential of 8 mV. All experiments were performed at 9.3°C. Most of the analysis presented here was performed, for computational purposes, on a patch with exactly one channel. It was verified, as discussed below, in other patches.

The experimental protocol and method of data acquisition are described in Horn et al.

(1984). In all experiments in this and the following paper, we low-pass-filtered the command voltage with a single-pole filter set at 2 kHz. Capacity transients were usually almost completely eliminated by subtraction at the level of the headstage (Hamill et al., 1981). In some cases, residual transients were removed by averaging records without openings and subtracting the average from each record in the series. If measurable, leakage currents were removed by an analog circuit. All records were filtered at 1.5 kHz by an eight-pole Bessel filter and were digitized at rates of 5.26–8.33 kHz.

Data Analysis

"Idealized" records were obtained from the digitized current records by setting a threshold for a transition (either opening or closing) at half the amplitude of the open channel current (Colquhoun and Sigworth, 1983). We tested the ability to resolve transitions by sampling filtered voltage pulses of known duration. When sampling at the lowest rate used in this paper (5.26 kHz), the minimal detectable duration was 150 μs. Since the single channel currents were at least seven times greater in amplitude than the rms baseline noise (see below), 150 μs was also the effective minimal duration of detectable openings.

The idealized records, then, were vectors of integers, representing the number of open channels at each epoch (time point) during a voltage pulse. Although the storage of these digitized records used a large amount of disk space, we found that this format was very useful for subsequent data analysis, especially for the maximum likelihood analysis discussed below.

Amplitude Histograms

After filtering single channel currents at a bandwidth of 1.5 kHz and sampling at a rate of 5.26 kHz, the records of the one-channel patch were cut into segments. Each segment represented, by the half-amplitude criterion (see above), current from either an open or a closed channel. Segments of <1 ms duration were discarded. The mean of each segment was subtracted from each sample point and amplitude histograms of open and closed channels were obtained as deviations from the mean. We also obtained histograms of the mean currents for each segment. For Gaussian noise, the error in estimation of the mean and mean square error requires that each segment be greater than ~0.8/bandwidth = 533 μs (Bendat and Piersol, 1971). The error in estimating the mean in this case is <1%.

The amplitude histograms of deviations from the mean are estimates of a probability density that we have plotted in bin widths of 9.8 or 12.6 fA (Fig. 9). The standard deviation of the number of observations in each bin is the square root of the number of observations since their distribution is approximately Poisson. Theoretical Gaussian functions were fitted to the amplitude histograms using a nonlinear least-squares fit with the Powell (1978) algorithm.

Exponential Fits to Open Time Histograms

Histograms of channel open time were fit with single exponentials by minimizing the chi-square values derived from a comparison of the data with the integral of the theory for each bin (Colquhoun and Sigworth, 1983). Both the time constant and the amplitude of the exponential were allowed to be free parameters. The width of each bin was the sampling interval (0.12–0.19 ms), except that bins containing less than five observations were combined. The first one or two bins were not used for exponential fitting to reduce errors from missed brief openings.

Maximum Likelihood Analysis

The method for obtaining estimates of parameters (i.e., rate constants and initial conditions) for linear kinetic models from idealized records has been described previously (Horn and Lange, 1983; Horn et al., 1984). We have extended the analysis in order to be able to use branched and cyclic kinetic models. In the most general model possible, any state can interconvert directly into all other states. This model was never used in practice, because the rate constants are not identifiable in highly cyclic models (Nguyen and Wood, 1982). For many of the cyclic models used here, the rate constants are not all independent parameters, but are functions of the others by microscopic reversibility. These rate constants were considered in the calculation of the likelihoods. Because of the computational time for our calculations, the models were restricted to five states, with each state being either open or closed. An examination of closing transitions (see Results) indicated that only a single open state was present in our data. Therefore, all the models had one open state and at most four closed states. We quickly found that more closed states were needed to adequately fit the activation time course. Since this was computationally infeasible, we usually truncated the beginning of the idealized records, a technique sometimes used in fitting macroscopic currents (e.g., see Neumcke et al., 1976). The implications of this truncation are discussed in the Results. For analysis of the experiment shown in Fig. 1, 1.33 and 0.76 ms were removed from the initial part of the idealized records at −40 and −25 mV.

We used a variable metric method (Powell, 1978) to search the likelihood surface. The algorithm, kindly provided by Dr. Kenneth Lange (University of California at Los Angeles), quickly and consistently found the maximum log(likelihood), which was independent of the initial guesses of parameters. It also produced an information (i.e., Hessian) matrix (Rao, 1973; Colquhoun and Sigworth, 1983). In some models, this matrix was singular and could not be inverted to yield a covariance matrix. This was observed in some of the cyclic models and suggested that some of the estimated parameters were not identifiable and could be expressed as linear combinations of others. In this case, we obtained a reduced covariance matrix by sweeping the information matrix in order of the tolerance of each parameter until the remaining parameters failed to pass the tolerance test (see discussion in Dixon, 1983). This procedure allowed us to obtain estimates of standard errors for identifiable parameters. Correlation matrices were generated from the reduced covariance matrices by dividing each term by the product of the standard errors of the estimates for the corresponding parameters.

For likelihood calculations, we used a VAX 11/730 computer (Digital Equipment Corp., Marlboro, MA) with an attached array processor (FPS 100; Floating Point Systems, Beaverton, OR). The array processor produced a 20- to 30-fold increase in computational speed. With these improvements, the estimation of all 11 parameters of the general model (see below) required ~20 h of computer time for 474 records containing 224 epochs each from our single channel patch. Models with fewer parameters required from 20 min to 12 h, depending on the initial guesses for the parameters. Records from patches with more channels required much more time to analyze. Consequently, we examined fewer models in those experiments. Table V lists all experiments in which maximum likelihood estimates of rate constants were obtained.

Likelihood ratio tests were applied to test hypotheses under nested conditions (Rao, 1973; Horn and Lange, 1983). A chi-square value is given by twice the difference between the maximum log(likelihood)s for the two models being compared. The number of degrees of freedom is the difference between the number of free parameters in each model. Note that in many of the tests below (e.g., in Table IV), the rate constants were estimated at

two voltages, which doubles the number of free parameters and therefore the degrees of freedom.

In patches with more than one channel, we also used a maximum likelihood method to estimate the number of channels (cf. Patlak and Horn, 1982). Usually the estimates were identical to the maximum number of channels simultaneously open.

Predicting Channel Properties from Transition Rate Constants

The probability that a channel is open as a function of time after a voltage step and the predicted probability densities (histograms) for channel open time, closed time, time to first opening, and burst duration were calculated numerically from the rate constants estimated by maximum likelihood analysis. A typical kinetic model used for these calculations is the basic model (scheme 1, shown below). At 50-μs intervals, the probability was computed that a channel entered each state, based both on its probability distribution among the states at the preceding interval and on the rate constants for transitions between states (e.g., see Horn and Lange, 1983). The initial distribution of channels among states was set appropriately for each theoretical density, and appropriate states were made absorbing. For example, the open time density is calculated by assuming that the channel is open at time zero and that all closed states are absorbing. The probability of the channel leaving the open state thereafter, $dP_{open}(t)/dt$, estimates the open time density (see discussion in Colquhoun and Hawkes, 1981; Horn, 1984). For the burst duration density, the theoretical prediction is complicated by the fact that if a channel closes to C_3, the closed state preceding the open state in the basic model, it sometimes reopens and the time spent in the closed states is considered part of the burst, but it sometimes inactivates, in which case the time spent in the closed states before inactivating is not part of the burst. This ambiguity was resolved by weighting the time spent in the set of closed states by the probability that a channel in a closed state would reopen rather than inactivate (i.e., rate($C_3 \rightarrow$ O)/[rate($C_3 \rightarrow$ O) + rate($C_3 \rightarrow$ I)]), where I represents a closed-inactivated state in the basic model. Because a channel in any of the closed states must ultimately reopen or inactivate through these pathways from C_3, the weighting factor is appropriate for all the closed states. The probability densities were scaled according to the method of Colquhoun and Sigworth (1983). The first one or two bins (0.19–0.38 ms) were not included in the scaling for open or closed times to minimize errors caused by brief missed transitions. We did not scale the probabilities of a channel being open [$P_{open}(t)$] and of a channel being open given that a burst started at time zero [$M(t)$], except to consider the number of channels.

RESULTS

Before examining possible kinetic models of sodium channel gating, we will address the question of the appropriateness of Markov models. Since the gating is so complex, we cannot answer this question completely, but instead we present evidence that the process of the closing of open channels has all the qualitative and quantitative aspects of a time-homogeneous Markov process, at least within the voltage range we have examined.

In order to simplify the analysis, we have restricted most of our observations to a patch containing only one channel. Records from this patch are displayed in Fig. 1. Each column shows a series of consecutive current records in response to 44-ms voltage steps (indicated by an arrow) to either −40 or −25 mV. By convention, a downward transition indicates an opening. A total of 474 and 426 records were obtained at −40 and −25 mV, respectively. Openings of duration

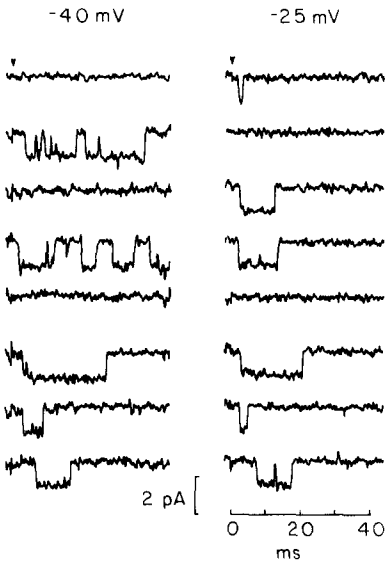

FIGURE 1. Currents from a patch with one channel. Consecutive current records from 44-ms voltage steps (indicated by an arrow) to −40 (left) and −25 mV (right). Note the multiple reopenings of the channel, especially at −40 mV. Voltage steps from the holding potential of −90 mV were preceded by a 20-ms prepulse to −120 mV. The interpulse interval was 1.5 s.

>150 μs were clearly resolved (see Methods), and transitions were measured using the half-amplitude threshold criterion of Colquhoun and Sigworth (1983). The following analysis was based on the idealized records from this and other experiments (see Methods).

The Sodium Channel Has One Open State

A true Markov process is said to be memoryless. That is, the dwell time in a given state does not depend upon the time when the state was entered; nor does it depend on the pathway by which it leaves this state. A necessary and sufficient condition for memorylessness is that the dwell time in such a state be exponentially distributed (Feller, 1971). We have examined the open times, and the histograms are well fit by a single exponential at each membrane potential. This is shown in Fig. 2 for an experiment with a two-channel patch, and in Fig. 4 for our one-channel patch. In the former experiment, the proportion of overlapping openings was 6% (−50 mV), 8% (−40 mV), and 17% (−25 mV). The quality of the fit suggests that sodium channels have a single open state (see also Fukushima, 1981; Quandt and Narahashi, 1982; Horn and Standen, 1983; Huang et al., 1984; however, see the contradictory evidence of Nagy et al., 1983). The theoretical curves in Fig. 2 were derived by minimizing the chi-square values obtained by comparison of theory with the data. Chi-square goodness-of-fit tests show that the histograms are well fit (see figure legend).

We were concerned, however, that this analysis might not reveal subtleties caused by the presence of more than one open state. Two alternatives were

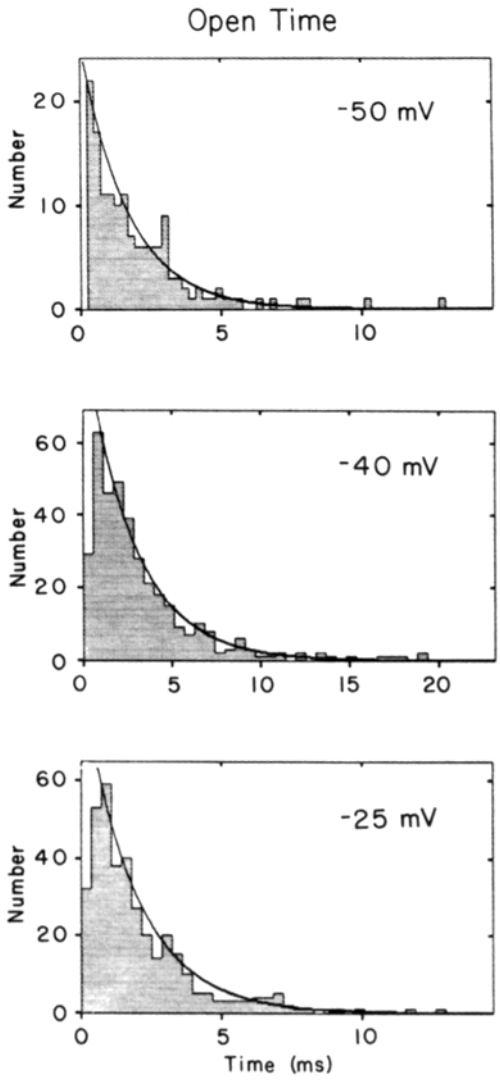

FIGURE 2. Histograms of open time from a patch with two channels. The exponential fit, obtained by minimizing chi-square values comparing the data with theory, gave mean open times of 1.7 (−50 mV), 2.7 (−40 mV), and 1.9 ms (−25 mV). The chi-square values (degrees of freedom) were 9.9 (19), 15.4 (29), and 36.0 (31) at −50, −40, and −25 mV, respectively, giving P values of 0.98, 0.98, and 0.25. Open times obtained by the maximum likelihood method (Horn and Standen, 1983) were 2.1 (−50 mV), 2.9 (−40 mV), and 1.9 ms (−25 mV).

considered. First, the open times may be nonstationary, as suggested for sodium currents in the node of Ranvier by autocovariance measurements (Sigworth, 1981) and by single channel data obtained from neuroblastoma cells (Nagy et al., 1983). These data could indicate the presence of more than one open state, with longer open times later in the pulse. If the same were happening in our

experiments, and the open times were not very different, the discrepancy may have been lost in the process of combining all the data into one histogram. The second alternative is that the sodium channel might contain more than one open state, but all states would have the same mean open time. In this case, the data of Sigworth could be explained, for example, if a channel opening early in the pulse would not tend to reopen after closing, whereas the late openings would be more "bursty," tending to reopen more often.

We have tested these alternatives for the one-channel patch (Fig. 1) in the following manner. The open times were ordered according to when the channel opened after the onset of the voltage step. The time, $t_{1/2}$, was obtained, which represented the time before which one half of the openings occurred, and cumulative open time histograms were plotted for openings occurring before and after $t_{1/2}$, as shown in the uppermost panels of Fig. 3. Qualitatively, open times early and late in the pulse are indistinguishable at both −40 and −25 mV. The density histograms were compared using Pearson's chi-square test for homogeneity of parallel samples (Rao, 1973, p. 399). The chi-square (degrees of freedom) values were 22.26 (34) and 17.40 (27) at −40 and −25 mV, which suggests there is no difference between the distributions of early and late open times ($P > 0.9$). This result was not appreciably altered by deliberately varying $t_{1/2}$.

The second alternative, that channels have more than one open state, each with the same dwell time, was tested in several ways. First, we measured burst durations at early and late times after the onset of the activating depolarization. We defined the beginning of a burst as the time of the first opening, and the end of the burst as that of the last closing during a 44-ms voltage pulse. If the channel was open at the end of the pulse, this time was considered the end of the burst. The latter occurred in, at most, 4.8% of the records. As above, bursts were ordered according to the time of their onset and separated into two equal-numbered groups. The cumulative distributions of burst durations early and late in the pulse are shown in the middle panels of Fig. 3. As in the case of open times, burst durations are quantitatively not dependent on when they begin. The chi-square test for homogeneity in this case gave values of 9.19 (20) and 15.08 (22) at −40 and −25 mV ($P \sim 0.98$ and ~ 0.85). This result was not affected by the possible truncation of bursts that occurred later in the pulse, since truncated density histograms of burst durations were also statistically indistinguishable.

We have also estimated the probability $M(t)$ of a channel being open, given that a burst started at time zero. This was obtained by averaging the idealized records, arranged so that the bursts all began at the same time (Neher and Steinbach, 1978; Horn and Lange, 1983). The bottom row of Fig. 3 shows that these conditional probability estimates, which are analogous to the nonstationary autocovariance measurements of Sigworth (1981), are also not dependent on the time when the bursts begin. The standard error bars in the lowermost panels of Fig. 3 were obtained by the use of Eq. 6.72 in Bendat and Piersol (1971, p. 183).

Four further arguments also support the idea that sodium channels have one open state. (*a*) We find no evidence for multiple conductance levels (see Fig. 10, below), which, in neuroblastoma cells, have been reported to correlate with

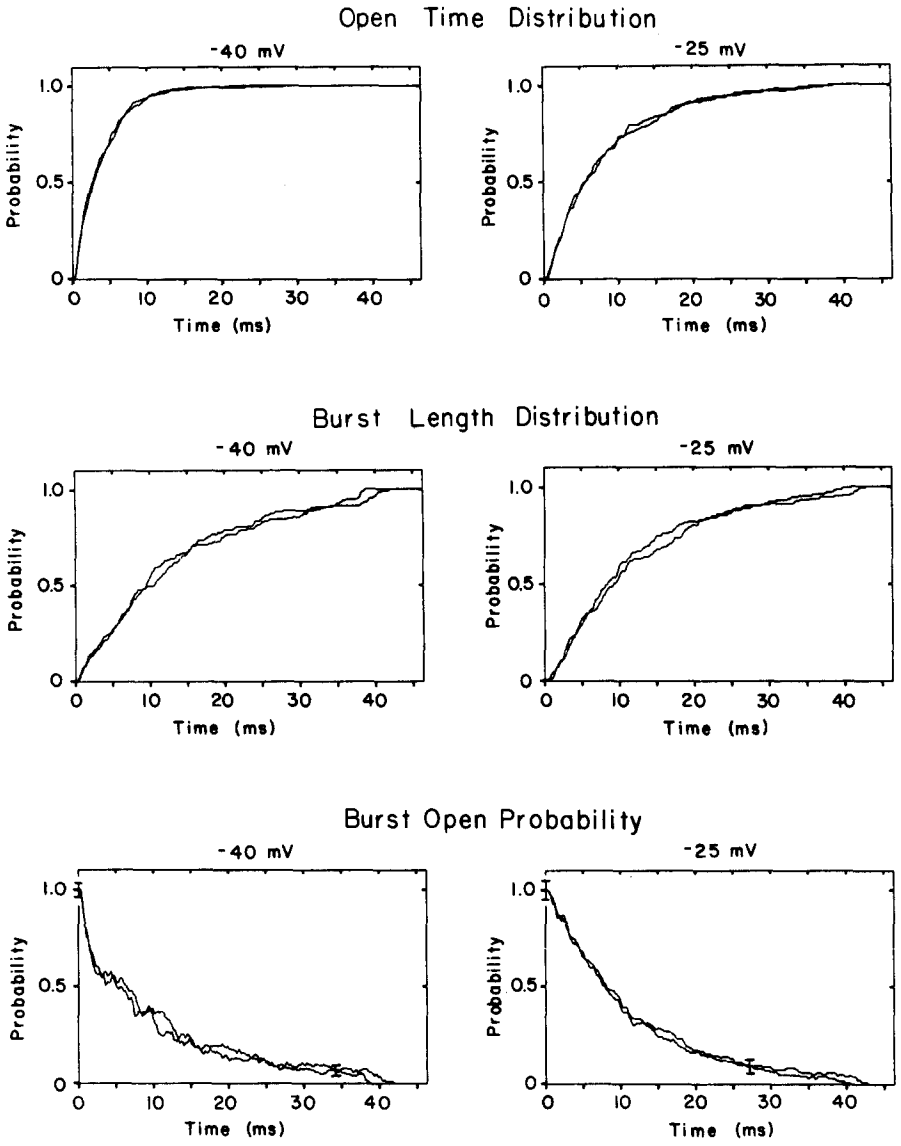

FIGURE 3. Comparison of opening statistics at early and late times in the record. Open time, burst duration, and probability of being open after the start of a burst, $M(t)$, vs. time are plotted for events occurring early and late in the record (see text).

multiple open times (Nagy et al., 1983). (*b*) For a single open state, the mathematical convolution of the distribution of first latencies (the times of the first opening after the voltage step) with $M(t)$ (the probability of being open during a burst) will reproduce $P_{open}(t)$, the probability of a channel being open after the voltage step (Aldrich et al., 1983). This prediction is confirmed in the following paper (Vandenberg and Horn, 1984). (*c*) The open time apparently does not depend on how the channel reached the open state. This has been experimentally

verified for *N*-bromoacetamide-treated single channels, in which the open times do not depend on the voltage preceding a step to −30 mV (Horn et al., 1984). (*d*) Finally, our analysis (Vandenberg and Horn, 1984) shows that channels can close by two different pathways. This means that the open time does not depend on the closing pathway, a possibility in a semi-Markov process (Feller, 1971).

Therefore, we are confident, at least under the conditions of our experiment, that sodium channels have a single, kinetically distinct open state. However, at more depolarized voltages, where the currents are more poorly resolved, we sometimes observed a low percentage of openings of exceptionally long duration (Horn et al., 1984). This raises the possibility that at depolarized potentials, a second open state may exist. A thorough examination of this possibility will require the use of pulses of longer duration, in order to allow the detection of a slow tail in the open time distribution.

A Kinetic Model

The number and arrangement of closed states of the sodium channel are not known (Armstrong, 1981; French and Horn, 1983). It is not even clear whether other transitions in the gating process are Markovian, although the large temperature dependence of the time course of activation argues in favor of this idea (Bezanilla and Taylor, 1978; Horn, 1984). Because of this ambiguity, specific kinetic models are always somewhat arbitrary. Within the limitations of our analysis, however, we have tested 25 Markov chain models with up to five states that are arranged in a variety of ways. These models can be compared statistically, as we will demonstrate below. For the sake of illustration, we will show an example of our statistical procedure using the following model, based partly on kinetic schemes found in Bezanilla and Armstrong (1977), Armstrong and Bezanilla (1977), and Armstrong and Gilly (1979). Later we will verify that this model is statistically superior to most alternatives. The "basic model" is

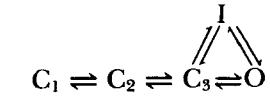

(Scheme 1)

There are three closed states, C_1, C_2, and C_3, one open state, O, and a closed-inactivated state, I. The inactivated state differs from the other closed states in two ways. First, channels at the holding potential tend to be in one of the other closed states. Second, the rates for leaving I are small at activating voltages. In other words, channels at rest tend to be in one of the closed states, and after a depolarization they eventually end up in the inactivated state. We have arbitrarily truncated the early portions of the current records by shifting the time origin of the data to improve the fit to the rising phase of the averaged records (see Methods), and we have made the assumption that at time zero, when the pulse begins, 98% of the channels are in C_1 and 2% are in C_2. These assumptions point out three difficulties with our analysis. First, there must be more than three closed states preceding the open state in the activation pathway. Second, the analysis gives little information about transitions that are several steps away from the open state (Horn and Lange, 1983). Finally, we are not certain about the

initial probability distribution among the states at rest. The initial distribution can be estimated, however, in two ways—either directly (Horn et al., 1984) or by extrapolation of estimated rate constants to prepulse voltages by assuming an exponential dependence on membrane potential. In the latter case, parameter estimates for nontruncated data (see Table II in Vandenberg and Horn, 1984) predict that the initial probabilities of being in states C_1 and C_2 are ~0.94 and ~0.05.

Note also that the model contains neither resting inactivation nor hibernating states (Horn et al., 1984), which means that the channel is always capable of opening during a voltage pulse. In this experiment, this seems a reasonable assumption, based on four arguments. First, a 20-ms prepulse to −120 mV preceded each depolarization. This should remove any resting fast inactivation at the −90-mV holding potential (see Horn et al., 1984; Vandenberg and Horn, 1984). Second, a runs analysis (Horn et al., 1984) failed to show convincing evidence for hibernation, which is a tendency for openings in successive records to be clustered at either −40 (P ~0.3) or −25 mV (P ~0.17). Experimentally, the interpulse interval was made as long as practically possible, 1.5 s, to avoid inducing slow inactivation or hibernation. Third, the peak probabilities of a channel being open during a voltage step (Fig. 6) were approximately the same as those estimated by the peak conductance-voltage relationship in macroscopic currents (Fig. 9 in Vandenberg and Horn, 1984). Finally, inclusion of hibernation in the analysis did not significantly improve the fits (see Discussion).

With the above limitations in mind, we have estimated rate constants for the basic model at both voltages for our one-channel patch, using the maximum likelihood method (see Methods). The rate constants are shown in Table I. Note that the model has 10 rate constants, although only 9 are estimated. The remaining rate constant is obtained from microscopic reversibility. The final fit was independent of the initial guesses, which indicates the smoothness of the likelihood surface (Horn and Lange, 1983). The estimates of rate constants entering and leaving the open state and that for inactivating from C_3 had relatively small standard errors. Transitions further from the open state were less well characterized.

One problem with this type of analysis is that it is difficult to speak about the "truthfulness" of any given model (cf. Leamer, 1983). However, we have adopted two strategies for assessing the quality of particular models. The first is to see how well they can make testable predictions, and the second is to compare and rank (if possible) models against one another. Several predictions of the basic model are shown in Figs. 4–7. We will discuss model comparisons later.

Fig. 4 plots the predicted and measured histograms of open and closed times. Data for the latter were obtained by measuring intervals between closings and subsequent openings. Since channels rarely reopened at −25 mV (Fig. 7; see also Vandenberg and Horn, 1984), the data here are sparse for closed times. The fits are all satisfactory.

Fig. 5 plots the predicted and observed burst open probability [i.e., $M(t)$] and burst duration histogram, and Fig. 6 plots the first latency histogram and $P_{open}(t)$. Finally, Fig. 7 plots the discrete probability distribution of the number of

TABLE I

Rate Constants and Correlation Coefficients for the Basic Model

Basic model:

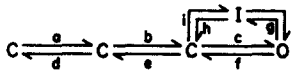

	Rate constant (s^{-1})*	
	−40 mV	−25 mV
a	1,260±1,710	1,190±253
b	1,420±1,830	1,240±269
c	438±60	772±75
d	768±895	0
e	729	0
f	246±15	31.2±3.5
g	7.6±11.7	82.5±5.1
h	1.3±0.7	0.12±0.04
i	256±38	242±31

Correlation matrix, −40 mV

	a	*b*	*c*	*d*	*f*	*g*	*h*	*i*
a	1.0	−0.95	0.78	−0.58	0.10	−0.12	−0.09	0.74
b		1.0	−0.82	0.79	−0.11	0.13	0.05	−0.79
c			1.0	−0.57	−0.08	0.10	−0.14	0.77
d				1.0	−0.09	0.12	−0.10	−0.58
f					1.0	−0.78	0.26	0.32
g						1.0	−0.33	−0.40
h							1.0	0.14
i								1.0

Correlation matrix, −25 mV

	a	*b*	*c*	*f*	*g*	*h*	*i*
a	1.0	−0.79	−0.23	0.01	−0.01	−0.01	−0.17
b		1.0	−0.24	0.01	−0.01	−0.02	−0.18
c			1.0	−0.11	0.08	−0.04	0.52
f				1.0	−0.22	0.38	0.13
g					1.0	−0.26	−0.09
h						1.0	0.36
i							1.0

* Standard errors of estimates are given for all identifiable parameters (see Methods). In some cases, the best estimate was zero, the minimal possible value.

openings per record, along with the predicted distribution. The latter was obtained as follows.

Since the mean dwell time in state I is estimated to be >740 ms (see Table I), considerably longer than the pulse duration of 44 ms, state I may be considered an absorbing state. With this simplification, we first calculate the probability P_1 of exactly one opening in a burst, defined here as the sequence of openings and closings in any record with at least one opening. It suffices to examine only part

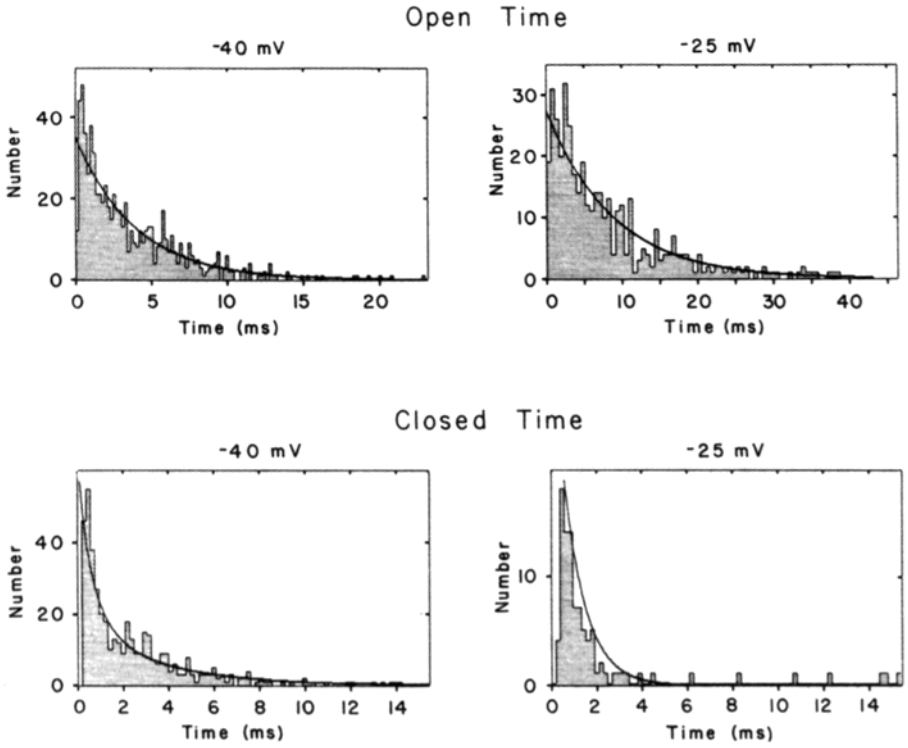

FIGURE 4. Comparisons of predictions of the basic model with data for open and closed times. The mean open times predicted by the basic model were 3.9 ± 0.2 (−40 mV) and 8.8 ± 0.4 ms (−25 mV). An exponential fit to the data (not shown), minimizing chi-square, gave comparable mean open times of 3.6 and 8.2 ms, with chi-square values (degrees of freedom) of 56.8 (45) and 66.9 (54) at −40 and −25 mV (*P* values, 0.12 and 0.12).

of the kinetic scheme in the basic model.

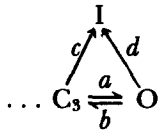

The rate constants a, b, c, and d completely characterize the distribution of the number of openings in a burst. In this scheme, P_1 = Prob (one opening in a burst) = Prob (channel reaches I before reopening) = Prob ([channel closes by $O \rightarrow C_3$ and does not reopen] $\cup$ [channel inactivates directly by $O \rightarrow I$]) = Prob [(channel closes by $O \rightarrow C_3$) $\cap$ (channel inactivated by $C_3 \rightarrow I$)] $\cup$ (channel inactivates directly by $O \rightarrow I$) = $b/(b + d) \times c/(a + c) + d/(b + d) = \epsilon$. Notice that if the channel closes via $O \rightarrow C_3$, it may dwell in C_3 for any length of time and may leave and re-enter C_3 from the left any number of times. The only relevant information here is the relative probability of $C_3 \rightarrow I$ vs. $C_3 \rightarrow O$.

If P_i is the probability of exactly i openings in a burst, then it has a geometric

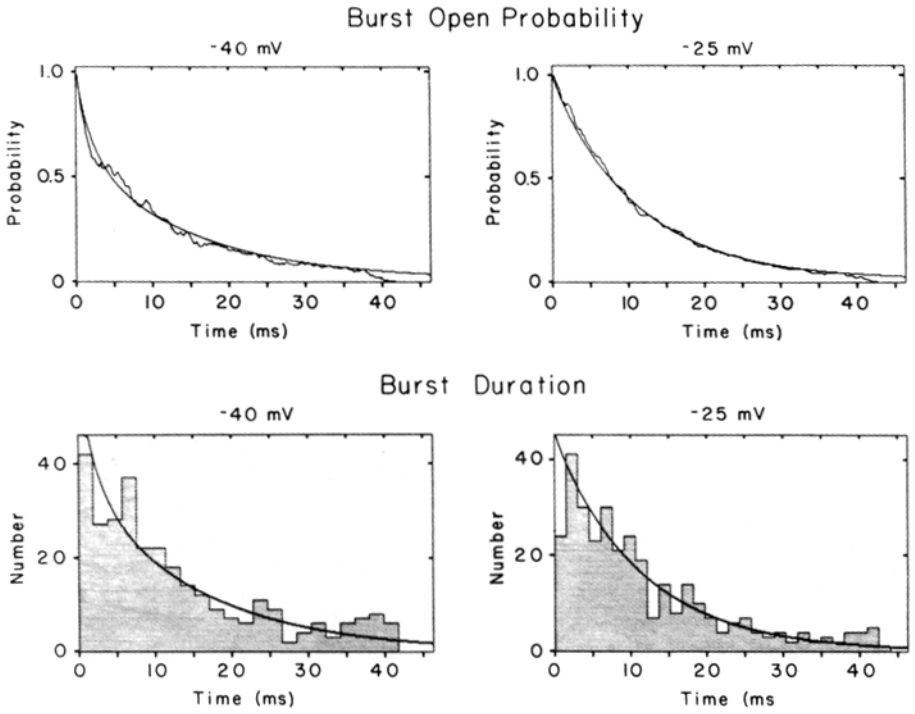

FIGURE 5. Comparisons of predictions of the basic model with data for burst duration and the probability of being open after the start of the burst, $M(t)$.

probability distribution

$$P_i = \epsilon(1 - \epsilon)^{i-1}, \qquad i = 1, \ldots, \infty$$

and the average number of openings in a burst is ϵ^{-1} (Colquhoun and Hawkes, 1981). We must also consider the probability of a channel never opening, $\gamma = c/(a + c)$. Then the modified probability distribution shown in Fig. 7 is given by P_i^*, where i is the number of openings per record, and

$$P_0^* = \gamma$$

$$P_1^* = (1 - \gamma)P_1$$

$$P_2^* = (1 - \gamma)P_2, \text{ etc.}$$

All of the above predictions are qualitatively consistent with the measurements derived from the data. We stress that the theoretical curves in Figs. 4–7 are not fits to the histograms, but were obtained entirely from the rate constants in Table I, which were extracted from the observed transitions themselves. The theoretical curves were not arbitrarily scaled.

Alternative Hypotheses

Within the limits of less than six states, one being open, there are many other possible alternative models. Table II shows the 25 models we have examined, in

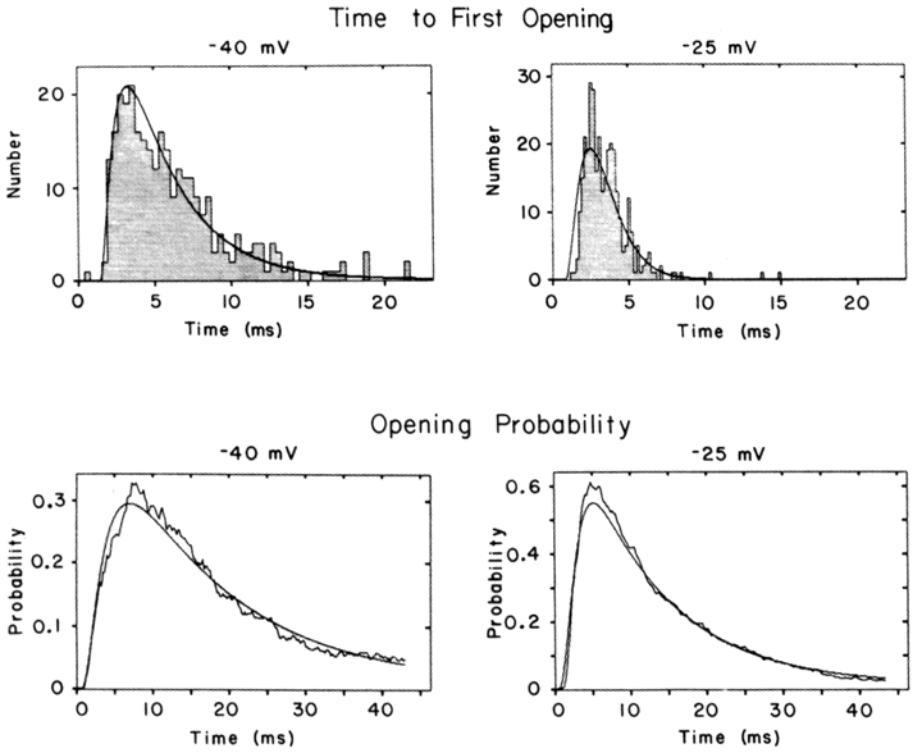

FIGURE 6. Comparisons of predictions of the basic model with data for first latency density and $P_{open}(t)$, the probability of the channel being open after the depolarizing voltage step.

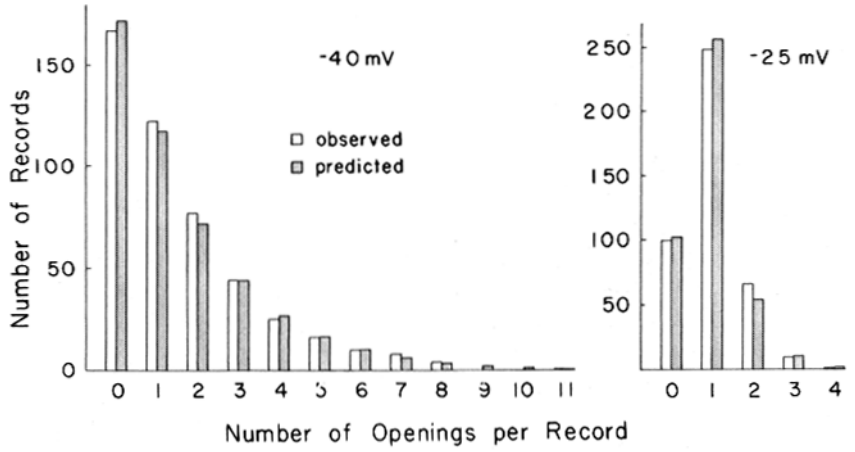

FIGURE 7. Comparisons of predictions of the basic model with data for number of openings per record.

TABLE II

Kinetic Models

Model number		Log (likelihood)	Number of parameters	AIC rank*
(1)‡	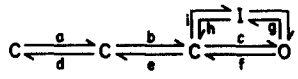	−10,351.55	10	2
(2)		−10,355.64	11	5
(3)	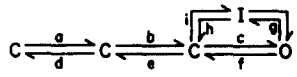	−10,356.61	9	3
(4)	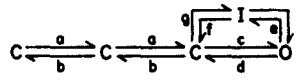	−10,356.93	7	1
(5)	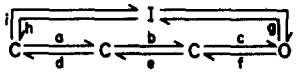	−10,358.83	9	4
(6)	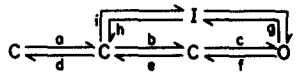	−10,361.24	9	6
(7)	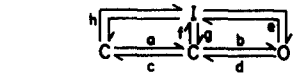	−10,380.45	8	8
(8)	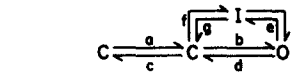	−10.380.45	7	7
(9)	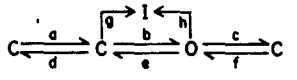	−10.385.18	8	9
(10)	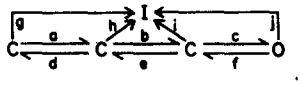	−10,418.99	10	16
(11)	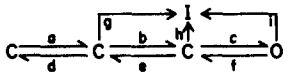	−10,419.98	9	15
(12)	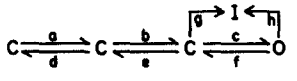	−10,420.66	8	14
(13)§	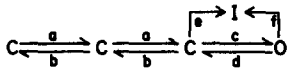	−10,420.78	7	12
(14)	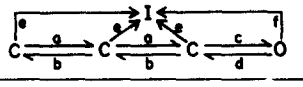	−10,421.20	6	10

TABLE II—*Continued*

Model number		Log (likelihood)	Number of parameters	AIC rank*
(15)	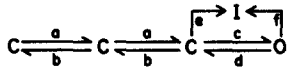	−10,421.43	6	11
(16)	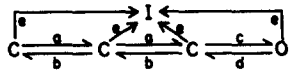	−10,424.84	5	13
(17)	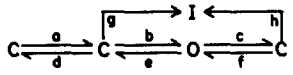	−10,432.60	8	17
(18)	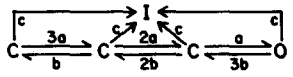	−10,462.27	3	18
(19)	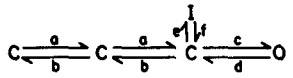	−10,490.37	6	19
(20)	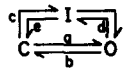	−10,573.18	5	20
(21)	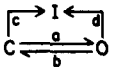	−10,595.38	4	21
(22)	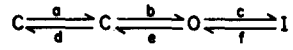	−10,691.50	6	22
(23)	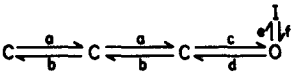	−11,265.29	6	24
(24)	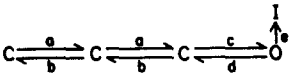	−11,265.29	5	23
(25)	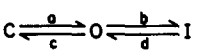	−11,613.18	4	25

* The AIC ranking orders the models by their Akaike information criterion value. The lowest number is considered best.

‡ An additional parameter, j, is the initial distribution of channels between the two closed states on the left.

§ An additional parameter, g, is the probability that a channel is hibernating at the beginning of the voltage pulse.

order of decreasing maximum log(likelihood). Some models had fewer than five states. Since the number of states in a model will directly affect the value of the likelihood (Horn and Lange, 1983), we used the following strategy to avoid this problem. Suppose that we desire to examine the three-state linear scheme

$$C \rightleftharpoons O \rightleftharpoons I.$$

We start with a five-state linear scheme,

$$C_1 \rightleftharpoons C_2 \underset{\beta}{\rightleftharpoons} C_3 \rightleftharpoons O \rightleftharpoons I,$$

setting the rate constant β equal to zero and the initial condition that the channel be in state C_3 with probability 1. This effectively reduces the number of states without reducing the number of compositions in the likelihood calculation (Horn and Lange, 1983).

Many of the alternative hypotheses are subhypotheses of model 2, which we call the general model. These models can be compared with the general model, using the likelihood ratio test (Rao, 1973; Horn and Lange, 1983), which provides a method for a statistical ranking of the subhypotheses. Table III gives the parameter estimates and correlation matrices for the general model, and

TABLE III

Rate Constants and Correlation Coefficients for the General Model

General model:

	Rate constant (s^{-1})	
	−40 mV	−25 mV
a	1,080±3,640	1,160±360
b	1,490±4,510	1,200±266
c	528	819±190
d	1,125	0
e	776±779	0
f	193±23	29.1±6.6
g	60.3±22.5	84.5
h	16.9	185±181
i	0.06	0.08±0.11
j	166.5	52.5
k	91.8	32±263

Correlation matrix, −40 mV

	a	*b*	*e*	*f*	*g*
a	1.0	−0.998	−0.96	0.89	−0.93
b		1.0	0.98	−0.88	0.92
e			1.0	−0.80	0.83
f				1.0	−0.92
g					1.0

Correlation matrix, −25 mV

	a	*b*	*c*	*f*	*h*	*i*	*k*
a	1.0	−0.55	−0.73	0.64	0.71	0.70	−0.73
b		1.0	−0.09	−0.003	−0.03	−0.02	0.03
c			1.0	−0.81	−0.87	−0.88	0.90
f				1.0	0.87	0.89	−0.88
h					1.0	0.97	−0.99
i						1.0	−0.97
k							1.0

TABLE IV

Comparison of Models: Likelihood Ratio Tests

General hypothesis: model 2

Subhypothesis model number	X^2	Degrees of freedom*	Approximate *P* value
3	1.93	4	0.75
4	2.58	8	0.96
5	6.38	4	0.2
6	11.21	4	0.025
10	126.69	2	$<10^{-4}$
11	128.67	4	$<10^{-4}$
12	130.04	6	$<10^{-4}$
14	131.11	10	$<10^{-4}$
15	131.57	10	$<10^{-4}$
16	138.40	12	$<10^{-4}$
18	213.25	16	$<10^{-4}$
19	269.46	10	$<10^{-4}$
23	1,819.29	10	$<10^{-4}$
24	1,819.30	12	$<10^{-4}$

General hypothesis: model 3

Subhypothesis model number	X^2	Degrees of freedom*	Approximate *P* value
4	0.65	4	0.96
12	128.11	2	$<10^{-4}$
15	129.64	6	$<10^{-4}$
19	267.54	6	$<10^{-4}$
23	1,817.36	6	$<10^{-4}$
24	1,817.37	8	$<10^{-4}$

General hypothesis: model 10

Subhypothesis model number	X^2	Degrees of freedom*	Approximate *P* value
11	1.98	2	0.4
12	3.35	4	0.5
14	4.43	8	0.8
15	4.88	8	0.8
16	11.71	10	0.3
18	86.57	14	$<10^{-4}$
24	1,692.61	10	$<10^{-4}$

* The number of degrees of freedom is two times the difference between the number of parameters in the models being compared because likelihoods for data from both −25 and −40 mV are combined (Horn and Lange, 1983).

Table IV gives the chi-square values for several possible likelihood ratio tests. We will address the topic of model comparisons in the Discussion.

We conclude this section by showing that the likelihood ratio criterion is a far better discriminator between models than the qualitative fits to histograms and conditional probabilities. Fig. 8 shows a comparison at −40 mV of the basic model, the Hodgkin-Huxley model, and a strictly coupled model. The Hodgkin-

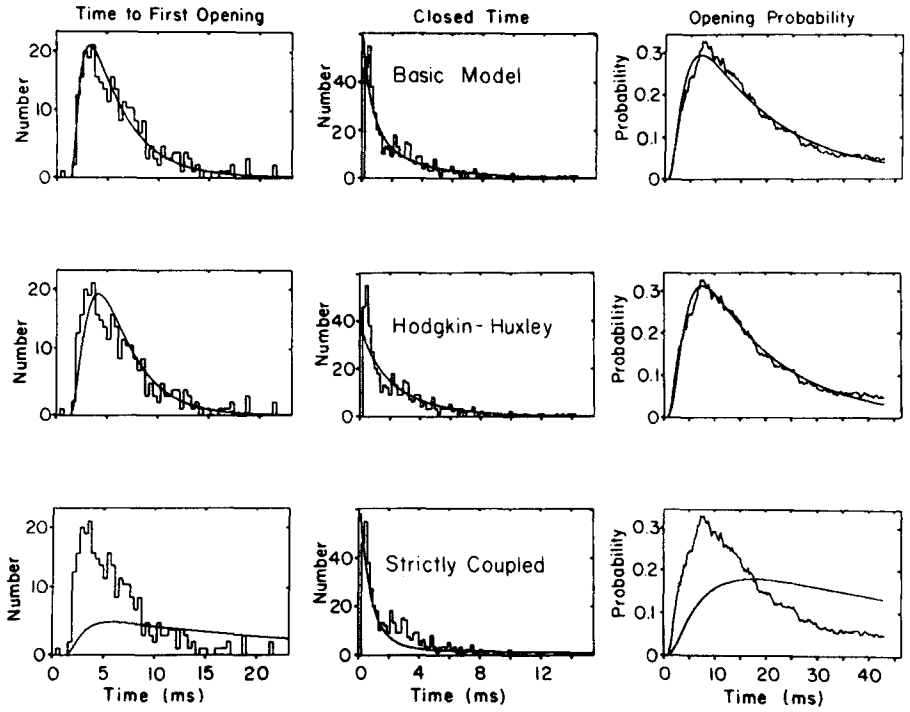

FIGURE 8. Comparisons of the basic model with the Hodgkin-Huxley (model 18) and strictly coupled (model 23) models for data at −40 mV. The rate constants for the Hodgkin-Huxley model determined by maximum likelihood analysis were α_m = 346.91, β_m = 65.37, and β_h = 68.72 s^{-1}.

Huxley model had three parameters, α_m, β_m, and β_h, which were estimated by our maximum likelihood procedures, assuming that $\alpha_h = 0$. We have plotted the first latency and closed time histograms, as well as $P_{open}(t)$ in Fig. 8. The theoretical open time histograms were identical for the three models. Qualitatively, at least, the Hodgkin-Huxley model produces theoretical curves that are reasonable fits to the measured data, although it tends to underestimate the number of brief closed durations. The predictions of the strictly coupled model (23 in Table II) are obviously poor representations of the data. The likelihood ratio test that compares these three models with the general model gives chi-square (and corresponding degrees of freedom) values of 1.93 (4), 213.25 (16), and 1,819.29 (10) for the basic, Hodgkin-Huxley, and strictly coupled models, respectively, with corresponding P values of 0.75, $<10^{-4}$, and $<10^{-4}$. The basic model is therefore vastly superior to both of the other models on statistical grounds, at least by comparison with the general model.

The above analysis is an example from a single patch with a single channel. Because of the computational demands of our maximum likelihood analysis, we have done most of our hypothesis testing on this experiment. Usually, patches have more than one channel, which greatly increases the computer time for calculations. In all, we analyzed four experiments in detail with this method. The

patches had up to four channels. Usually the basic model, or some simplification of it, produced reasonable fits to our data and was always statistically comparable or superior to the alternatives we examined (see Table V below). As in the example presented here, we always found that rates entering and leaving the open state were better determined than other rates in the process. Further details of the analysis of this and other experiments are given below and in Vandenberg and Horn (1984).

Frequency Limitations

The maximum likelihood analysis assumes perfect data, i.e., no missed transitions. The effect of missed transitions on parameter estimation is unclear and almost certainly depends on the kinetic model. Transitions could be missed in two ways. First, a very short event (e.g., an opening) of full amplitude could be missed because of an insufficient sampling rate used for digitizing the current record. Second, an event could have such a short duration that it will be reduced by the low-pass filter to a peak level below that of the half-amplitude threshold criterion (see Methods).

The first problem was addressed by Horn and Lange (1983), who showed that a conservative sampling rate that will not affect estimates is $>10\ Nk_i$, where k_i is the largest rate constant in the model and N is the number of channels. In the above experiments, the sampling rate was 5.26 kHz. Therefore, rate constants greater than $\sim 526\ s^{-1}$ are probably underestimated.

We have shown (see Methods) that the combination of filtering and sampling rate set an effective minimal detectable duration of 150 μs. If either open or closed times have significant components in this range, one might expect to see deviations from Gaussian amplitude distributions for open or closed channel currents (Sigworth, 1982; Auerbach and Sachs, 1983). Fig. 9 shows amplitude distributions of deviations of currents from mean values at −40 and −25 mV. At both voltages, the distributions are well fit by a Gaussian function, which is superimposed over the data. The standard deviation of the current noise is 0.15–0.16 pA, rms. This compares with a theoretical minimum of 0.05 pA for a noiseless headstage amplifier with a 10-GΩ feedback resistor and an infinite seal resistance. In agreement with this, we found no evidence for a high proportion of unresolved brief openings. Typically, open times were exponentially distributed with a mean open time of ~2.0 ms. The probability of an opening of <150 μs in such a process is <0.08. The estimated proportions of missed brief openings for the open time histograms shown in Fig. 4 are 0.04 and 0.02 at −40 and −25 mV. Note, however, that occasional missed closings are also reflected in overestimates of the open time, which can modify the above conclusions.

Fig. 9 shows that slight deviations from the Gaussian function occur for closed channels at −40 mV and for open channels at both voltages (see arrows). These deviations might be expected for a small percentage of missed openings at −40 mV and missed closings at both potentials. Note that the mean open time is smaller at −40 mV (Fig. 4). Such events may be missed by our threshold criterion, but are reduced in amplitude by the 1.5-kHz filter. Unresolved closings could

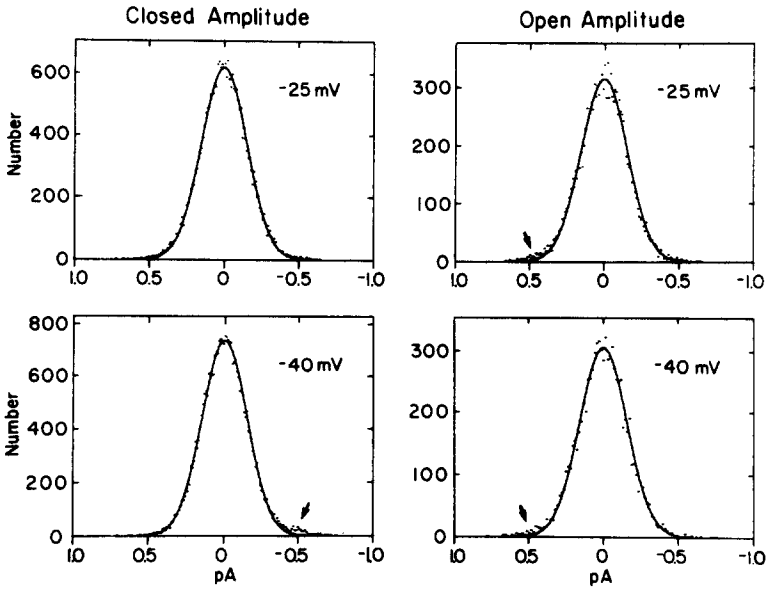

FIGURE 9. Amplitude histograms of deviation from mean current for open and closed channels. The Gaussian curves fitted to the data have standard deviations of 0.15 (closed channel current, −40 and −25 mV) and 0.16 pA (open channel current, −40 and −25 mV).

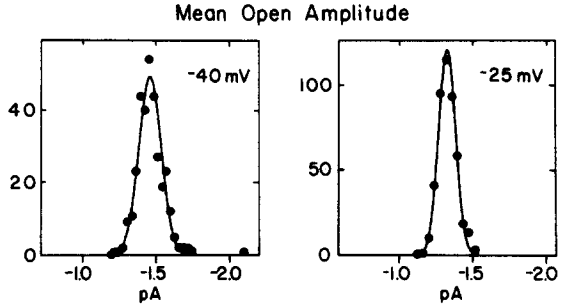

FIGURE 10. Amplitude distributions of mean open amplitudes. The mean single channel amplitudes were 1.46 (−40 mV) and 1.32 pA (−25 mV), and standard deviations were 76 (−40 mV) and 58 fA (−25 mV).

account, for example, for the paucity of brief events in the closed time histograms in Fig. 4.

Fig. 10 plots histograms of mean amplitude for open events of >1 ms duration. These histograms show no evidence of multiple conductance levels, in agreement with experiments using neuroblastoma cells (Huang et al., 1984; however, see Nagy et al., 1983).

DISCUSSION

In this paper, we have examined the use of time-homogeneous Markov chain models to describe the gating kinetics of sodium channels. Such models are

appropriate when the dwell time in each state is exponentially distributed. This was substantially verified for the open state within the voltage range we have studied (−50 to −25 mV). Furthermore, we find no evidence for the possibility of multiple open states, each with the same mean lifetime. Our results are not in agreement with those of Sigworth (1981), who found that autocovariance measurements of sodium currents in frog node of Ranvier were decidedly nonstationary; the relaxations were faster immediately after an activating depolarization than they were later on. We can think of three possible reasons for the discrepancy. The first is simply a preparation difference. One obvious difference between our two preparations is that the inactivation time course for single pulse measurements in frog node is multiexponential (Chiu, 1977), whereas it is well described by a single exponential curve in GH_3 cells (Fernandez et al., 1984; Vandenberg and Horn, 1984). It is possible that a slow process exists in frog node that corresponds to slow relaxations later in the pulse. The second possibility is the voltage range. We have only examined the range negative to −20 mV, whereas Sigworth measured autocovariance near 0 mV. At the more depolarized voltages, we have seen some evidence of exceptionally long openings (unpublished observations; also see Horn et al., 1984). At voltages beyond the range of the usual patch recording experiments (greater than +20 mV), Chandler and Meves (1970) found a noninactivating component to sodium current in perfused squid axons. They ascribed this to a second open state with slower kinetics. Although we find no evidence for such a process in macroscopic sodium currents (Vandenberg and Horn, 1984), it is possible that the sodium channels have a second open state at more depolarized voltages, or else that sodium channels are sufficiently heterogeneous that they do not all have the same open time. Note that nonexponential open time distributions have been observed in multichannel patches from mammalian cells (Patlak and Horn, 1982; Aldrich et al., 1983; Nagy et al., 1983). Some caution is required in the interpretation of such data because of the sampling errors inherent in handling overlapping openings (Patlak and Horn, 1982; Horn and Standen, 1983). Furthermore, heterogeneity in the population of channels may produce nonexponential histograms. The third possibility is that we have not used pulses of sufficient duration to detect occasional, very long openings. If such events occur, they are either very rare in our experiments or else open at very late times after a depolarization.

Although channel closing conforms with predictions of a Markov process in our experiments, we have little information about other gating transitions. A number of arguments have been advanced to suggest that these processes, too, are Markovian (Colquhoun and Hawkes, 1983; French and Horn, 1983; Horn, 1984).

Models of Gating

We have estimated rate constants for several Markov models, limited to at most five states, using a maximum likelihood method. One of the principal values of this approach is the possibility of comparing models statistically with likelihood ratio tests (Rao, 1973; Horn and Lange, 1983). This is possible, however, only for models in which one is a smoothly parameterized subhypothesis of the other,

i.e., when the models are nested. Many of the models in Table II, however, are not comparable in this way. For example, the only difference between models 19 and 23 is that in the former, only state C_3 can inactivate; in the latter, only the open state can inactivate. Both models have the same number of parameters and are subhypotheses of the basic model (model 3). However, they are not properly compared by the likelihood ratio test since one is not a subhypothesis of the other. The former model (19) is clearly better, however, as shown by a comparison of their respective log(likelihood)s (Table II).

Akaike (1974) has proposed a method for ranking non-nested hypotheses. He introduced an "asymptotic information criterion" (AIC) of the following form:

$$\text{AIC} = 2[\text{number of parameters} - \log(\text{maximum likelihood})].$$

The model with the minimum AIC is considered best. Although this approach has not been universally accepted (e.g., Leamer, 1983), it allows for a simple ordering of models and has the added advantage that it favors parsimonious models. Table II shows the ordered AIC ranking for the 25 models examined. The best model by this criterion is model 4, which is the basic model (model 3) constrained to have equal rate constants for the first two transitions. Table IV shows that this model is statistically indistinguishable from either the general model (model 2) or the basic model (3) under a likelihood ratio test. This test also shows it to be indistinguishable from model 1 (chi-square = 10.76; degrees of freedom = 6, $P \sim 0.1$), which is the basic model with an extra parameter for the estimation of the initial condition (see Table II).

An examination of the AIC ranking in Table II and the likelihood ratio tests in Table IV leads to the following general observations, which are readily verified by examination of these two tables.

(*a*) The best models require inactivation to occur from both the open state and at least one closed state. The log(likelihood)s are not significantly increased by allowing inactivation to occur from more than one closed state. Based on the relative values of the maximum log(likelihood)s of models 3, 5, and 6, inactivation from the state preceding opening produces a slightly better model than inactivation from another closed state does. However, it is not clear whether the difference between these models is significant, since all three are statistically indistinguishable from the general model (model 2) and their maximum likelihoods are within 5 log units of one another. Models 3, 4, 8, 12, 13, 15, 19, and 22–25 are all variations on this theme of inactivation occurring near the open state, and are consistent with the notion of a coupling between activation and inactivation, as we will explore in the following paper (Vandenberg and Horn, 1984).

(*b*) The models are significantly improved by allowing inactivation to be reversible. For example, an irreversible version of the basic model is model 12. Table IV shows that the latter is markedly inferior ($P < 10^{-4}$). This is generally true for comparisons between reversible and irreversible versions of the same model.

(*c*) The AIC ranking shows that inactivation from one closed state only (model 19) is statistically superior to the strictly coupled model 23, in which inactivation

can occur only from the open state. All strictly coupled models (22–25), which require a channel to open before inactivating, produced very poor predictions of channel properties. This is probably due to difficulty in simultaneously fitting the brief first latencies with the sizable proportion of blank records. In a strictly coupled model, a blank record indicates that the channel is closed but not inactivated.

(*d*) The log(likelihood)s in this experiment are not significantly increased by the inclusion of a hibernating state (see Horn et al., 1984). This is seen by a comparison of models 13 and 15. A likelihood ratio test here gives a P value of ~0.6. In other experiments, however (see Vandenberg and Horn, 1984), hibernation was apparent in the raw data, and the log(likelihood)s were increased by its inclusion in the model (Table V).

(*e*) If the basic model is given the added freedom of estimating the initial probability distribution between the first two closed states at the onset of the depolarization, model 1 results. Although this model has the highest likelihood of all models, it is not statistically distinguishable from model 4 ($P \sim 0.1$), in which the initial probability distribution is fixed (see Methods). By the AIC, it also ranks below the much simpler model 4.

(*f*) The more closed states the better. Although models with two closed states (e.g., models 7 and 8) did surprisingly well, in terms of the magnitudes of their maximum log(likelihood)s, this was primarily due to the fact that we truncated the beginning of the records in this experiment (see Methods). For nontruncated data from the same experiment, models with three closed states were vastly superior to those with two closed states (unpublished observation).

(*g*) The irreversible Hodgkin-Huxley model (model 18) is statistically inferior to most other irreversible models with the same number of states (with the exception of strictly coupled models). Note that the reversible version of this

TABLE V

Models Fit by the Maximum Likelihood Analysis

Experiment	Number of channels	Voltage	Number of records	Ranking
		mV		
28	4	−20	219	
		−30	201	13 < 15 < 24
		−40	283	
		−50	261	
50	2	−40	314	15 < 13 < 18 < 21* < 21
56	1	−25	426	See Table II
		−40	474	
67	2	−25	474	
		−40	475	4* < 10 < 13 < 21* < 21
		−50	333	

The ranking refers to model numbers listed in Table II, and is given in order of best to worst model according to the AIC criterion. Model numbers followed by an asterisk correspond to the model numbers in Table II with the addition of a hibernating state. For experiments with more than one channel, a hibernating state usually improved the fit. Experiment 56 is the one-channel patch analyzed in Tables I–IV.

model could not be tested, because it has eight states (e.g., see French and Horn, 1983), which is beyond the range of our analysis.

The preceding discussion demonstrates our ability to compare and eliminate alternative hypotheses. As mentioned earlier, we could confine ourselves to the question of how well an individual model makes predictions. However, we have generally found that most of the models examined yielded similar predictions for a variety of histograms (e.g., see Fig. 8). The only models that produced exceptionally poor predictions were three-state models and strictly coupled models (models 20–25). These models also had the lowest likelihoods. The problem of discriminating between kinetic models that yield similar predictions has been encountered in several studies of gating (e.g., see Conti et al., 1980; Sigworth, 1981). One option is to say that such models cannot realistically be discriminated. Our opinion, however, is that hypothesis testing is a desirable possibility, using the likelihood method. In many cases, we were able to quantitatively compare two models using a likelihood ratio test.

Evaluation of the Method

We have adopted a fundamentally different approach to model development than that usually used for kinetic analysis of gating. Usually a "synthetic" approach rather than a "statistical" approach is taken (Armstrong, 1981). The former strategy involves the construction of conceptually reasonable models with a minimal number of parameters, which are estimated in a semiquantitative manner by comparing the predictions of the model with the data. Often the comparisons are qualitative and only permit nonrigorous comparisons between models. Such an approach might not, for example, be able to distinguish between the Hodgkin-Huxley and a statistically superior model (Fig. 8).

The approach we use, by comparison with other methods of both synthetic and statistical varieties, has a few notable advantages and several disadvantages, which we will discuss briefly. Further discussion of the merits and problems of this method can be found in Horn and Lange (1983). The principal advantage is the power to estimate parameters and test hypotheses, as we have shown above. It also has the important advantage over many other methods for the analysis of single channel data of being able to handle nonstationary data in patches with more than one channel. One of the main reasons for the power of this method is that all the data are evaluated simultaneously. For example, the approach of fitting histograms by sums of exponentials (e.g., see Colquhoun and Sigworth, 1983) will produce estimates of eigenvalues for the kinetic model of choice, but reliable strategies for choosing appropriate conditional histograms and extracting the underlying rate constants are not available. In our data, for example, the closed time histogram at −25 mV (Fig. 4) has very few elements, since the channel rarely reopens after closing. If we fit this to a sum of four exponential components, appropriate for the basic model, the values of the four time constants would be much less reliable than the one time constant obtained by a fit to the open time histogram. We are unaware of a rigorous method to weight the reliability of the fits of these two histograms in the effort to extract rate constants from them. Another general problem with the use of histograms is that

they lump data and thus lose information about detailed relationships between events. For example, an open time histogram loses information about relative patterns of long- and short-duration openings (Jackson et al., 1983). This problem does not occur in our likelihood analysis, because the data remain in a relatively "raw" form, which preserves all of the detailed relationships between observable transitions.

One of the strengths of this method is the ability to determine standard errors of parameter estimates. Unfortunately, the standard errors are sometimes larger than the values of the estimates themselves (see Tables I and III). Although this may be construed as a criticism of the method, we believe that it demonstrates the real difficulty in estimating parameters in a cyclic compartment model in which only transitions into and out of one state can be observed directly. This problem cannot be fully appreciated in the synthetic approach to understanding gating. It further demonstrates why many methods cannot successfully discriminate between models.

It is worth considering the sensitivity of this method in estimating rate constants for branched kinetic sequences. (Horn and Lange [1983] already addressed this issue using linear sequences.) We therefore simulated single channel currents for model 15 of Table II. We generated 500 records for a single channel using rate constants similar in value to those obtained in our experiments, and sampled these records every 190 μs. The rate constants used for the simulation were (see Table II): $a = 1{,}000$, $b = 200$, $c = 500$, $d = 200$, $e = 250$, and $f = 40\ s^{-1}$. The estimated rate constants obtained from the simulated data were $\hat{a} = 985 \pm 73$, $\hat{b} = 148 \pm 53$, $\hat{c} = 443 \pm 36$, $\hat{d} = 177 \pm 11$, $\hat{e} = 218 \pm 21$, and $\hat{f} = 46.9 \pm 8.7\ s^{-1}$, which are in reasonable agreement with the values used for the simulation and again support the reliability of our analysis. These estimates were marginally improved by reducing the sampling interval to 100 μs.

The principal drawback of the likelihood method is the extensive time required for calculations. The estimates of rate constants for one model can take several days of computer time for a five-state model in the case of a four-channel patch, using our VAX computer with a dedicated array processor (see Methods). Because the analysis is so time-consuming, we have had to restrict our detailed attention to relatively few patches having a minimal number of channels (Table V). If channels are sufficiently heterogeneous, we may be drawing conclusions from a biased sample. In the following paper (Vandenberg and Horn, 1984), this point is addressed by comparing the analysis of several patches with macroscopic currents.

Another drawback of the method is that it requires that the currents be well resolved within the frequency bandwidth of interest. Therefore, the amplitude of transitions should be well above the background noise. Although this may be possible for sodium channels, at least over part of the voltage range of activation, many channel types, such as calcium channels (Hagiwara and Ohmori, 1983) or acetylcholine receptor channels (Colquhoun and Sakmann, 1981; Auerback and Sachs, 1983), have rapid transitions within the frequency range of interest.

This paper demonstrates that the likelihood technique, which has previously been used for relatively simple problems of single channel data analysis, is a

powerful approach in the kinetic analysis of voltage-gated sodium channels. The following paper (Vandenberg and Horn, 1984) exploits this method in an examination of inactivation and its relationship with activation.

We are grateful to Dr. Kenneth Lange for modifying our maximum likelihood program to allow for the analysis of branching and cyclic kinetic schemes and to Dr. Elliot Landaw for suggesting the method of obtaining a reduced covariance matrix. Drs. Francisco Bezanilla and Joseph Stimers generously offered criticisms of the manuscript.
Supported by National Institutes of Health grants NS 703-01 and NS 186-08, and by National Science Foundation grant PCM 76-20605 to R.H. C.V. was supported by Muscular Dystrophy Association and National Institutes of Health postdoctoral fellowships.

Original version received 28 March 1984 and accepted version received 13 June 1984.

REFERENCES

Akaike, H. 1974. A new look at the statistical model identification. *IEEE Trans. Automatic Control.* AC-19:716–723.

Aldrich, R. W., D. P. Corey, and C. F. Stevens. 1983. A reinterpretation of mammalian sodium channel gating based on single channel recording. *Nature (Lond.).* 306:436–441.

Armstrong, C. M. 1981. Sodium channels and gating currents. *Physiol. Rev.* 61:644–683.

Armstrong, C. M., and F. Bezanilla. 1977. Inactivation of the sodium channel. II. Gating current experiments. *J. Gen. Physiol.* 70:567–590.

Armstrong, C. M., and W. F. Gilly. 1979. Fast and slow steps in the activation of sodium channels. *J. Gen. Physiol.* 74:691–711.

Auerbach, A., and F. Sachs. 1983. Flickering of a nicotinic ion channel to a subconductance state. *Biophys. J.* 42:1–10.

Bendat, J. S., and A. G. Piersol. 1971. Random Data Analysis and Measurement Procedures. Wiley-Interscience, New York. 407 pp.

Benzanilla, F. 1982. Gating charge movements and kinetics of excitable membrane proteins. *In* Proteins of the Nervous System: Structure and Function. B. Haber, J. R. Perez-Polo, and J. D. Coulter, editors. Alan R. Liss, Inc., New York. 3–16.

Bezanilla, F., and C. M. Armstrong. 1977. Inactivation of the sodium channel. I. Sodium current experiments. *J. Gen. Physiol.* 70:549–566.

Bezanilla, F., and R. Taylor. 1978. Temperature effects on gating currents in the squid giant axon. *Biophys. J.* 23:479–484.

Brodwick, M. S., and D. C. Eaton. 1982. Chemical modification of excitable membranes. *In* Proteins in the Nervous System: Structure and Function. B. Haber, J. R. Perez-Polo, and J. D. Coulter, editors. Alan R. Liss, Inc., New York. 51–72.

Chandler, W. K., and H. Meves. 1970. Evidence for two types of sodium conductance in axons perfused with sodium fluoride solution. *J. Physiol. (Lond.).* 211:653–678.

Chiu, S. Y. 1977. Inactivation of sodium channels: second order kinetics in myelinated nerve. *J. Physiol. (Lond.).* 273:573–596.

Colquhoun, D., and A. G. Hawkes. 1981. On the stochastic properties of single ion channels. *Proc. R. Soc. Lond. B Biol. Sci.* 211:205–235.

Colquhoun, D., and A. G. Hawkes. 1983. The principles of the stochastic interpretation of ion-channel mechanisms. *In* Single-Channel Recording. B. Sakmann and E. Neher, editors. Plenum Press, New York. 135–175.

Colquhoun, D., and B. Sakmann. 1981. Fluctuations in the microsecond time range of the current through single acetylcholine receptor ion channels. *Nature (Lond.).* 294:464–466.

Colquhoun, D., and F. Sigworth. 1983. Fitting and statistical analysis of single-channel records. *In* Single-Channel Recording. B. Sakmann and E. Neher, editors. Plenum Press, New York. 191–264.

Conti, F., B. Neumcke, W. Nonner, and R. Stampfli. 1980. Conductance fluctuations from the inactivation process of sodium channels in myelinated nerve fibres. *J. Physiol. (Lond.).* 308:217–239.

Dixon, W. J. 1983. BMDP Statistical Software. University of California Press, Berkeley, CA. 671–672.

Feller, W. 1971. An Introduction to Probability Theory and Its Applications. Volume II. John Wiley & Sons, New York. 669 pp.

Fernandez, J., A. P. Fox, and S. Krasne. 1984. Membrane patches and whole-cell membranes: a comparison of electrical properties in rat clonal pituitary (GH_3) cells. *J. Physiol. (Lond.).* In press.

Fishman, H. M., H. R. Leuchtag, and L. E. Moore. 1983. Fluctuation and linear analysis of Na-current kinetics in squid axon. *Biophys. J.* 43:293–307.

French, R. J., and R. Horn. 1983. Sodium channel gating: models, mimics, and modifiers. *Annu. Rev. Biophys. Bioeng.* 12:319–356.

Fukushima, Y. 1981. Identification and kinetic properties of the current through a single Na^+ channel. *Proc. Natl. Acad. Sci. USA.* 78:1274–1277.

Greeff, N. G., R. D. Keynes, and D. F. Van Helden. 1982. Fractionation of the asymmetry current in the squid giant axon into inactivating and noninactivating components. *Proc. R. Soc. Lond. B Biol. Sci.* 215:375–389.

Hagiwara, S., and H. Ohmori. 1983. Studies of single calcium channel currents in rat clonal pituitary cells. *J. Physiol. (Lond.).* 336:649–661.

Hamill, O. P., A. Marty, E. Neher, B. Sakmann, and F. J. Sigworth. 1981. Improved patch-clamp techniques for high-resolution current recording from cells and cell-free membrane patches. *Pflügers Arch. Eur. J. Physiol.* 391:85–100.

Horn, R. 1984. Gating of channels in nerve and muscle: a stochastic approach. *In* Ion Channels: Molecular and Physiological Aspects. W. D. Stein, editor. Academic Press, Inc., New York. In press.

Horn, R., and K. Lange. 1983. Estimating kinetic constants from single channel data. *Biophys. J.* 43:207–223.

Horn, R., and N. B. Standen. 1983. Counting kinetic states: the single channel approach. *In* The Physiology of Excitable Cells. A. Grinnell and W. Moody, editors. Alan R. Liss, Inc., New York. 181–189.

Horn, R., C. A. Vandenberg, and K. Lange. 1984. Statistical analysis of single sodium channels. Effects of *N*-bromoacetamide. *Biophys. J.* 45:323–335.

Huang, L.-Y. M., N. Moran, and G. Ehrenstein. 1984. Gating kinetics of batrachotoxin-modified sodium channels in neuroblastoma cells determined from single-channel measurements. *Biophys. J.* 45:313–322.

Jackson, M. B., B. S. Wong, C. E. Morris, H. Lecar, and C. N. Christian. 1983. Successive openings of the same acetylcholine receptor channel are correlated in open time. *Biophys. J.* 42:109–114.

Leamer, E. E. 1983. Model choice and specification analysis. *In* Handbook of Econometrics. Z.

Grilisches and M. D. Intriligator, editors. Elsevier/North-Holland Biomedical Press, Amsterdam. 1:285–330.

Nagy, K., T. Kiss, and D. Hof. 1983. Single Na channels in mouse neuroblastoma cell membrane. Indications for two open states. *Pflügers Arch. Eur. J. Physiol.* 399:302–308.

Neher, E., and J. H. Steinbach. 1978. Local anaesthetics transiently block currents through single acetylcholine-receptor channels. *J. Physiol. (Lond.).* 277:153–176.

Neumcke, B., W. Nonner, and R. Stampfli. 1976. Asymmetrical displacement current and its relation with the activation of sodium current in the membrane of frog myelinated nerve. *Pflügers Arch. Eur. J. Physiol.* 363:193–203.

Neumcke, B., W. Nonner, and R. Stampfli. 1978. Gating currents in excitable membranes. *Int. Rev. Biochem.* 19:129–155.

Nguyen, V. V., and E. F. Wood. 1982. Review and unification of linear identifiability concepts. *SIAM (Soc. Ind. Appl. Math.) Rev.* 24:34–51.

Patlak, J., and R. Horn. 1982. The effect of *N*-bromoacetamide on single sodium channel currents in excised membrane patches. *J. Gen. Physiol.* 79:333–351.

Powell, M. J. D. 1978. A fast algorithm for nonlinearity constrained optimization calculations. *In* Numerical Analysis. G. A. Watson, editor. Lecture Notes in Mathematics No. 630, Springer-Verlag, Berlin. 144–157.

Quandt, F. N., and T. Narahashi. 1982. Modification of single Na^+ channels by batrachotoxin. *Proc. Natl. Acad. Sci. USA.* 79:6732–6736.

Rao, C. R. 1973. Linear Statistical Inference and Its Applications. Second edition. John Wiley & Sons, New York. 625 pp.

Rubinson, K. A. 1982. The sodium current of nerve under voltage clamp has heterogeneous kinetics. A model that is consistent with possible kinetic behavior. *Biophys. Chem.* 15:245–262.

Sigworth, F. J. 1981. Covariance of nonstationary current fluctuations at the node of Ranvier. *Biophys. J.* 34:111–133.

Sigworth, F. J. 1982. Fluctuations in the current through open ACh-receptor channels. *Biophys. J.* 37:309*a*. (Abstr.)

Vandenberg, C. A., and R. Horn. 1984. Inactivation viewed through single sodium channels. *J. Gen. Physiol.* 84:535–565.

Yeh, J. 1982. A pharmacological approach to the structure of the Na channel in squid axon. *In* Proteins in the Nervous System: Structure and Function. B. Haber, J. R. Perez-Polo, and J. D. Coulter, editors. Alan R. Liss, Inc., New York. 17–49.